



Lack of monoacylglycerol lipase prevents hepatic steatosis by favoring lipid storage in adipose tissue and intestinal malabsorption^S

Matteo Tardelli,* Francesca V. Bruschi,* Thierry Claudel,* Claudia D. Fuchs,* Nicole Auer,* Victoria Kunczer,* Tatjana Stojakovic,[†] Hubert Scharnagl,[§] Aida Habib,^{*,**,+†} Gernot F. Grabner,^{§§} Robert Zimmermann,^{§§} Sophie Lotersztajn,^{**} and Michael Trauner^{1,*}

Hans Popper Laboratory of Molecular Hepatology,* Division of Gastroenterology and Hepatology, Department of Internal Medicine III, Medical University of Vienna, Vienna, Austria; Clinical Institute of Medical and Chemical Laboratory Diagnostics,[†] University Hospital Graz, Graz, Austria; Clinical Institute of Medical and Chemical Laboratory Diagnostics,[§] Medical University of Graz, Graz, Austria; INSERM-UMR1149,** Centre de Recherche sur l'Inflammation, Paris, France; Department of Biochemistry and Molecular Genetics,^{††} American University of Beirut, Beirut, Lebanon; and Institute of Molecular Biosciences,^{§§} University of Graz, Graz, Austria

ORCID IDs: 0000-0003-2232-7779 (M.T.); 0000-0002-5006-5473 (F.V.B.); 0000-0002-5601-9830 (T.C.)

Abstract Monoacylglycerol lipase (MGL) is the rate-limiting enzyme in the degradation of monoacylglycerols. To examine the role of MGL in hepatic steatosis, WT and MGL KO (MGL^{-/-}) mice were challenged with a Western diet (WD) over 12 weeks. Lipid metabolism, inflammation, and fibrosis were assessed by serum biochemistry, histology, and gene-expression profiling of liver and adipose depots. Intestinal fat absorption was measured by gas chromatography. Primary adipocyte and 3T3-L1 cells were analyzed by flow cytometry and Western blot. Human hepatocytes were treated with MGL inhibitor JZL184. The absence of MGL protected mice from hepatic steatosis by repressing key lipogenic enzymes in liver (Srebp1c, Ppar γ 2, and diacylglycerol O-acyltransferase 1), while promoting FA oxidation. Liver inflammation was diminished in MGL^{-/-} mice fed a WD, as evidenced by diminished epidermal growth factor-like module-containing mucin-like hormone receptor-like 1 (F4/80) staining and C-C motif chemokine ligand 2 gene expression, whereas fibrosis remained unchanged. Absence of MGL promoted fat storage in gonadal white adipose tissue (gWAT) with increased lipogenesis and unchanged lipolysis, diminished inflammation in gWAT, and subcutaneous AT. Intestinal fat malabsorption prevented ectopic lipid accumulation in livers of MGL^{-/-} mice fed a WD. In vitro experiments demonstrated increased adipocyte size/lipid content driven by PPAR γ .^{¶¶} In conclusion, our data uncover that MGL deletion improves some aspects of nonalcoholic fatty liver disease by promoting lipid storage in gWAT and fat malabsorption.—Tardelli, M., F. V. Bruschi, T. Claudel, C. D. Fuchs, N. Auer, V. Kunczer, T. Stojakovic, H. Scharnagl, A.

Habib, G. F. Grabner, R. Zimmermann, S. Lotersztajn, and M. Trauner. **Lack of monoacylglycerol lipase prevents hepatic steatosis by favoring lipid storage in adipose tissue and intestinal malabsorption.** *J. Lipid Res.* 2019. 60: 1284–1292.

Supplementary key words nonalcoholic fatty liver disease • monoacylglycerol lipase • obesity • lipolysis and fatty acid metabolism • nuclear receptors/peroxisome proliferator-activated receptor • adipocyte • adipocytes/obesity • fatty acid/metabolism

Nonalcoholic fatty liver disease (NAFLD) has become an important public health issue because of its high prevalence and association with adverse cardio-metabolic and hepatic outcomes (1). NAFLD spans a spectrum from simple hepatic steatosis through nonalcoholic steatohepatitis, ultimately leading to liver fibrosis, cirrhosis, and cancer (1–3). Hepatic triglyceride (TG) homeostasis is regulated by a complex interplay between plasma NEFA uptake and de novo lipogenesis, as well as FA oxidation and TG export by VLDLs. Hepatic steatosis develops when the rate of hepatic

Abbreviations: Aox, aldehyde oxidase; APC, adipocyte progenitor cell; AT, adipose tissue; Atgl, adipose triglyceride lipase; BOB, β -hydroxybutyrate; Ccl2, C-C motif chemokine ligand 2; Cd36, cluster of differentiation 36; Chol, cholesterol; Cpt1 α , carnitine palmitoyltransferase 1A; Dgat1, diacylglycerol O-acyltransferase 1; F4/80, epidermal growth factor-like module-containing mucin-like hormone receptor-like 1; gWAT, gonadal white adipose tissue; H&E, hematoxylin-eosin; HFD, high-fat diet; Hsl, hormone-sensitive lipase; MG, monoglyceride; MGL, monoacylglycerol lipase; NAFLD, nonalcoholic fatty liver disease; pio, pioglitazone; rosi, rosiglitazone; sWAT, subcutaneous white adipose tissue; TG, triglyceride; WD, Western diet.

¹To whom correspondence should be addressed.

e-mail: michael.trauner@meduniwien.ac.at

^S The online version of this article (available at <http://www.jlr.org>) contains a supplement.

Copyright © 2019 Tardelli et al. Published under exclusive license by The American Society for Biochemistry and Molecular Biology, Inc.
This article is available online at <http://www.jlr.org>

This work was supported by French National Research Agency Joint Grant ANR-15-CE14-003 (S.L.) and Austrian Science Fund Grant I2661 and F7310-B21 (M.T.).

Manuscript received 18 February 2019 and in revised form 2 May 2019.

Published, *JLR Papers in Press*, May 2, 2019

DOI <https://doi.org/10.1194/jlr.M093369>

FA input (uptake and synthesis) exceeds the rate of FA output (oxidation and secretion) (4). In addition, steatosis is associated with hepatic insulin resistance and thereby reduced sensitivity of the liver to the suppressive effects of insulin on the hepatic output of glucose.

Monoacylglycerol lipase (MGL) is the final enzymatic step of the TG degradation pathway and hydrolyzes monoglycerides (MGs) deriving from phospholipids or TGs into glycerol and FAs (5). Moreover, MGL notably hydrolyzes 2-arachidonoylglycerol, which is a potent ligand within the endocannabinoid system (6). Metabolic studies highlighted that hepatic levels of saturated and unsaturated species of MGs were highly increased in MGL^{-/-} mice, showing improved insulin sensitivity and glucose tolerance under a high-fat diet (HFD) (7). Although previous reports demonstrated that the absence of MGL protects from adipose tissue (AT) inflammation and insulin resistance, resulting in a leaner phenotype (7, 8), the molecular link between lipid products generated by MGL deficiency and observed metabolic changes remains largely unexplored. Importantly, it is unclear whether MGL has a functional role in the AT-liver axis in the background of obesity-associated hepatic steatosis. Therefore, we explored the role of MGL in hepatic steatosis induced by a Western diet (WD) challenge.

Here, we demonstrate that MGL deficiency prevented hepatic lipid accumulation induced by WD feeding. Mechanistically, increased gonadal white AT (gWAT) lipid storage in MGL^{-/-} mice prevented ectopic lipid accumulation in the liver, whereas intestinal malabsorption of FA species diminished body weight. In vitro, MGL-deficient adipocyte progenitor cells (APCs) showed increased lipid accumulation, and MGL was identified as a PPAR γ target in 3T3-L1 cells. Thus, targeting MGL action in vivo could provide a novel therapeutic strategy to combat obesity-associated hepatic steatosis and related metabolic complications.

METHODS

Animals and diet

Experiments were performed in 2-month-old male MGL^{-/-} mice and WT littermates (C57BL/6 background, n = 7 per group unless otherwise stated) weighing 20–25 g, generated by R. Zimmermann (8). Animals were housed in a 12 h light/dark house facility and fed ad libitum either a WD (Research Diet: D12079B, protein 17%, fat 40%, and carbohydrate 43%) or standard chow for 12 weeks; organ and blood collection were performed in the morning. The experimental protocols were approved by the local Animal Care and Use Committee (BMWF.66.009/0117-II/3b/2013), and routine serum biochemical analyses were performed as previously described (9).

Histology and immunohistochemistry

Mouse liver samples were fixed with neutral buffered 4% paraformaldehyde and subsequently paraffin embedded. Hematoxylin-eosin (H&E) staining and Sirius Red were performed in liver as described (10). Detection of the epidermal growth factor-like module-containing mucin-like hormone receptor-like 1 (F4/80) and Mac-2 were performed as previously described (11).

Isolation and culture of primary hepatocytes

Hepatocytes were isolated from normal liver tissue from surgical resections unsuitable for transplantation, approved by the ethics committee of the Medical University of Vienna (EK 2032/2013) using a protocol described elsewhere (12, 13). Hepatocytes were seeded on uncoated plastic dishes and cultivated with DMEM supplemented with 10% FBS and antibiotic (Gibco Life Technologies, CA). Cells were treated with an MGL inhibitor (JZL184, 1 μ M) for 24 h.

Primary APC and 3T3-L1 cell culture and adipocyte differentiation

gWAT tissue obtained from MGL^{-/-} mice and WT littermates (n = 4 per group) was minced with scissors and digested in adipocyte isolation buffer as previously described (14). Briefly, samples were incubated for 40 min at 37°C on a shaker, and the digested tissue was filtered and centrifuged. The pellet was resuspended and filtered through a 70 μ m and then 40 μ m cell strainer (14). The resulting mouse APCs were cultured in DMEM supplemented with 10 ng/ml recombinant basic human fibroblast growth factor (FGF β ; Gibco, CA) to maintain their self-renewal capacity and inhibit differentiation (15). To assess the adipogenic potential of APCs, cells were seeded to reach confluence and differentiated as follows: 3 days treatment with adipogenic medium (advanced DMEM, 5% heat-inactivated FBS supplemented with 20 μ g/ml insulin, 10 μ M dexamethasone, and 0.5 mM isobutylmethylxanthine) followed by 3 days of DMEM with 5% FBS and 20 μ g/ml insulin and 4 days of DMEM with 5% FBS. The 3T3-L1 cells were differentiated according to previously published works (16, 17). Cells were treated with an MGL inhibitor (JZL184, 1 μ M), rosiglitazone (rosi) alone, or in combination with GW9662 or pioglitazone (pio) for 24 h prior to harvesting.

Western blot

Whole-cell extracts were obtained using RIPA buffer (150 mM NaCl, 1% Triton X-100, 0.5% sodium deoxycholate, 0.1% SDS, and 50 mM Tris, pH 8.0) containing complete EDTA-free protease inhibitor cocktail tablets (Roche Diagnostics GmbH, Germany) and phosphatase inhibitors (20 mM β -glycerophosphate, 10 mM 4-nitrophenylphosphate, and 50 mM sodium vanadate; all Sigma-Aldrich). Primary Abs were diluted in 3% BSA TBS-Tween 1 \times solution at different concentrations, and SDS-PAGE was run as previously reported (12, 18). Proteins were detected by ECL chemiluminescence (GE Amersham, Arlington Heights, IL).

mRNA analysis and PCR

AT and liver were homogenized in TRIzol reagent (Invitrogen, Carlsbad, CA), and RNA was isolated and transcribed to cDNA according to the manufacturer's protocol. Gene expression was normalized to 18S and assessed by quantitative real-time RT-PCR on an ABI Prism 7000 cycler using commercial Assays-on-Demand kits (all Applied Biosystems, Foster City, CA).

Flow cytometry

For BODIPY lipid staining, 3T3-L1 cells and APCs were trypsinized, collected, and incubated with a working solution of 1 μ g/ml BODIPY 493/503 in PBS for 30 min at 37°C. Afterward, 5 μ g/ml propidium iodide (Sigma-Aldrich) was added to each tube for 5 min before flow cytometric analysis. The side scatter was used to detect changes in the cell granularity and the green fluorescence (525 nm) of BODIPY to measure the intracellular lipid droplet formation (19, 20). Flow cytometry was performed using BD FACSCANTO™ and BD FACSDIVA™ software (Becton Dickinson, NJ).

Determination of lipid absorption

For determination of lipid absorption, diets containing sucrose polybehenate (5% of total dietary fat content; wt/wt) were prepared and fed to mice for three consecutive days. Fresh fecal pellets were collected, extracted, and analyzed by gas chromatography of FA methyl esters as previously described (21). In brief, 10 mg feces and diet were extracted using chloroform/methanol (2/1), 1% acetic acid, and 500 mM butylated hydroxytoluene (BHT) for 1 h at room temperature. The aqueous phase was reextracted using chloroform and 500 mM BHT for 15 min at room temperature. The combined organic phases were evaporated under a stream of nitrogen and FA methyl ester were generated from whole lipid extracts using methanolic hydrogen chloride (22). Samples were reconstituted in 100 ml hexane and measured by gas chromatography-flame ionization detection. A wall-coated fused silica 25 m, 0.32 mm ID column (FFAB-CB for free FAs, Varian) was used. A total of 1 μ l of the sample was injected at an injector temperature of 230°C; column A: temperature gradient from 150°C (hold for 0 min) to 250°C (hold for 2 min) with 5°C·min⁻¹, and a second ramp to increase the temperature to 260°C (hold for 5 min) with 10°C·min⁻¹ was applied. Detector settings: base temperature, 200°C; ignition threshold, 0.2 pA; air flow rate, 200 ml·min⁻¹; H₂ flow rate, 30 ml·min⁻¹; and makeup, 20 ml·min⁻¹. The absorption of FAs was calculated from the ratios of behenic acid to other FAs in diet and feces (23).

Determination of TGs, glycerol, insulin, β -hydroxybutyrate, and FAs

Liver and plasma TG/glycerol content was determined according to manufacturer protocol and measured by using a commercially available enzymatic reagent, TGs FS (DiaSys, Diagnostic Systems, Germany). Mouse plasma insulin (Mercodia, Sweden) and β -hydroxybutyrate (BOB; Sigma-Aldrich) were measured with commercially available ELISA kits. FFAs were measured in stools; approximately 10 mg of feces was homogenized in a chloroform solution, and the organic phase was dried at 50°C and resuspended for colorimetric measurement according to manufacturer protocols (FFA quantification assay kit, Abcam, UK).

Serum adiponectin levels

Serum adiponectin levels were evaluated using a mouse adiponectin ELISA kit (Bio Vendor, Czech Republic).

Statistics

Data are shown as mean \pm SD. Statistical analysis was performed between two groups by Student's two-tailed *t*-test. For analysis of multiple measurements, we performed two-way ANOVA followed by Tukey post hoc test using GraphPad Prism version 7.00 for Windows (GraphPad Software, La Jolla, CA). A *p* value of 0.05 or less was considered to be statistically significant.

RESULTS

MGL deficiency protects from hepatic steatosis and weight gain favoring intestinal malabsorption

In order to assess the role of MGL in hepatic steatosis, WT and MGL^{-/-} mice were fed either chow or a WD for 12 weeks to induce obesity and steatosis. Notably, MGL deletion protected from weight gain (Fig. 1A, supplemental Fig. S1A) and hepatomegaly (as demonstrated by a decreased liver/body weight ratio; Fig. 1B) despite an increased gWAT/BW ratio (Fig. 1B) and unchanged food

intake (data not shown). This resulted in protective effects against hepatic steatosis upon WD challenge, as evidenced by reduced macrovesicular steatosis in H&E and diminished serum transaminases [alanine transaminase (ALT) and aspartate transaminase (AST)] and plasma TGs (Fig. 1C, D, Table 1). Moreover, fasting plasma NEFAs were significantly diminished in MGL^{-/-} animals (Table 1), in line with diminished lipolysis from adipose depots (24). Accordingly, total hepatic TG content showed decreased accumulation of lipids in MGL^{-/-} mice fed a WD (Fig. 1E). Next, we measured FFA amounts in stool, showing a slight increase already at baseline in MGL^{-/-} mice compared with WT, which was further exacerbated by the dietary challenge (Fig. 1F). To investigate this difference in FA output, we determined intestinal absorption of dietary fat using the nonhydrolyzable and nonabsorbable sucrose polybehenate as internal standard in the WD (21) as previously performed (23). We found significantly reduced lipid absorption in MGL^{-/-} animals compared with controls (Fig. 1G) with increased intestinal cholesterol (Chol) excretion (*Abcg5*) but unchanged *Abcg8* and other lipid transporters *Npc1l1*, *Srb1*, and cluster of differentiation 36 (*Cd36*) (supplemental Fig. S1C) in accordance with a previous report (25). This indicates that reduced lipid absorption also contributes to decreased obesity in MGL^{-/-} mice.

In line with reduced hepatic TG content, gene expression of key markers of FA synthesis such as *Srebp1c*, *Fasn*, and FA storage *Ppar γ 2* was down-regulated (Fig. 2A). Given the downregulation of hepatic *Ppar γ 2* mRNA expression, we next analyzed its transcriptional target diacylglycerol *O*-acyltransferase 1 (*Dgat1*), which catalyzes the formation of TGs from diacylglycerol and acyl-CoA (26). Notably, *Dgat1* expression was significantly downregulated together with *Cd36* in obese MGL^{-/-} mice (Fig. 2A). Western blot analysis, however, showed no statistically significant changes in PPAR γ 2 protein expression (Fig. 2B). mRNA levels of *Ppara α* , *carnitine palmitoyltransferase 1A (Cpt1 α)*, *PPARG coactivator 1 Alpha*, and *aldehyde oxidase (Aox)* increased (Fig. 2C), whereas *adipose triglyceride lipase (Atgl)*, *abhydrolase domain containing 5 (Cgi-58)*, and *hormone-sensitive lipase (Hsl)* diminished (Fig. 2D), suggesting an effect on FA metabolism. Genes involved in Chol synthesis were decreased for *sterol regulatory element binding transcription factor 2 (Srebf2)* and in trend for *3-hydroxy-3-methylglutaryl-CoA reductase (Hmgcr)* in MGL^{-/-} mice fed a WD (Fig. 2D). Plasma glycerol and insulin level significantly diminished, whereas ketone bodies remained unchanged, as shown by BOB measurement (Table 1). mRNA levels of *Foxo1*, as key regulators of hepatic gluconeogenesis, were significantly enhanced in obese WT livers, whereas the absence of MGL protected from WD-induced hepatic *Foxo1* upregulation (supplemental Fig. S1D). Expression of *Pepck*, a gene involved in gluconeogenesis, was decreased in obese MGL^{-/-} mice compared with WT (supplemental Fig. S1D). Intriguingly, primary hepatocytes treated with the MGL inhibitor JZL184 confirmed in vivo data, with a significant downregulation of *Ppar γ 2*, *Fasn*, and *Dgat1* gene expression (Fig. 2E). Collectively, these results suggest that the reduced hepatic TGs and intestinal loss of FAs could contribute to the

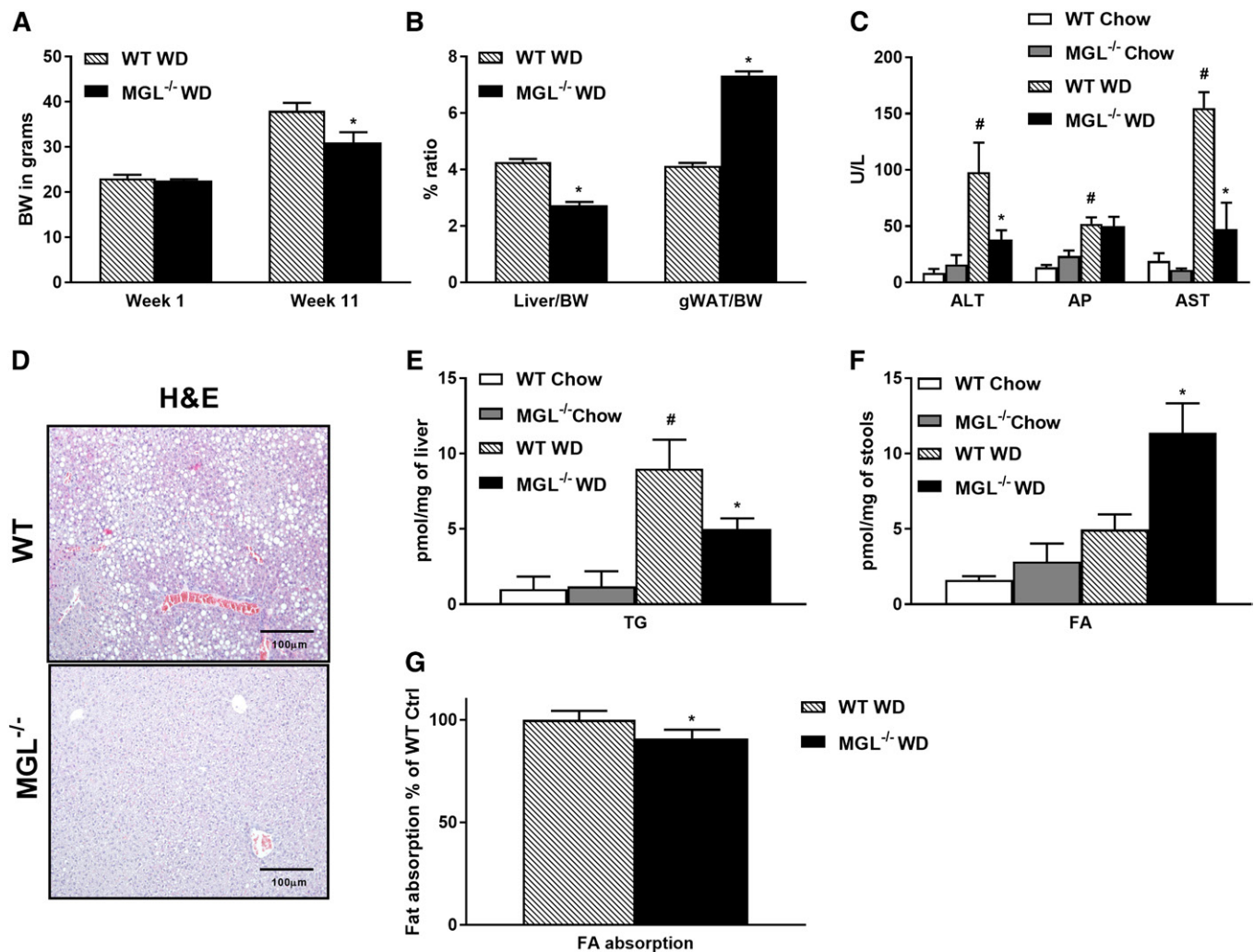


Fig. 1. MGL deficiency in mice protects from hepatic steatosis. WT and MGL^{-/-} mice were fed chow or a WD for 12 weeks (n = 7 per group). Mouse body weight (BW) (A) and liver/BW ratio was diminished in MGL^{-/-} mice fed a WD, whereas gWAT/BW increased (B). C: Serum liver enzymes (ALT and AST) were diminished in MGL^{-/-} mice. D: Representative H&E staining of liver paraffin sections demonstrates decreased steatosis. Hepatic TG content measured in tissue homogenates was less abundant in MGL^{-/-} mice fed a WD (E), whereas fecal FA levels increased (F). G: Fat absorption analyzed by gas chromatography of FA methyl esters was diminished in MGL^{-/-} WD versus WT WD (n = 4). White and gray bars, WT and MGL^{-/-} mice on chow diet; hatched and black bars, WT and MGL^{-/-} mice on WD. Ctrl, control. * P ≤ 0.05 WT WD versus MGL^{-/-} WD; # P ≤ 0.05 WT WD versus WT chow. Gene expression is shown as percentages relative to 18S.

diminished hepatic steatosis in MGL^{-/-} mice. Moreover, downregulation of hepatic gluconeogenic enzymes translates into beneficial effects of MGL deficiency on lipid homeostasis in obesity.

TABLE 1. Plasma metabolites and insulin levels in WT versus MGL^{-/-} mice fed a WD

	WT	MGL ^{-/-}
NEFA (mmol/l)	1.6 ± 0.1	0.86 ± 0.1*
TG (mg/dl)	51 ± 12	23 ± 2*
Chol (mg/dl)	159 ± 20	110 ± 12
Glycerol (mM)	0.3 ± 0.2	0.1 ± 0.1*
Insulin (µg/l)	4 ± 0.6	2.6 ± 0.2*
BOB (µmol/l)	0.1 ± 0.1	0.1 ± 0.2

Values were obtained from male mice receiving a WD for 12 weeks. Data are presented as mean ± SD (n = 5).

* P < 0.05.

MGL deletion ameliorates hepatic inflammation without affecting fibrosis

In order to evaluate the potential impact on hepatic inflammation, gene expression of proinflammatory markers was analyzed together with immunohistochemistry (IHC) for F4/80 in liver. Interestingly, hepatic gene expression of *C-C motif chemokine ligand 2 (Ccl2)* and *F4/80* were markedly increased in WD-fed WT, but not in MGL^{-/-}, animals (Fig. 2F). Furthermore, IHC analysis of liver sections showed a higher accumulation of macrophages in obese WT mice, but not in MGL^{-/-} mice (supplemental Fig. S1B). Fibrosis remained unchanged as evidenced by Sirius Red staining (supplemental Fig. S1B) and hepatic mRNA expression of *collagen type I alpha 1 chain* and *transforming growth factor beta 1 (Tgfβ)* (Fig. 2F). Taken together, these results reveal that MGL is a mediator of hepatic steatosis and inflammation, but not fibrosis, in obesity-driven inflammation.

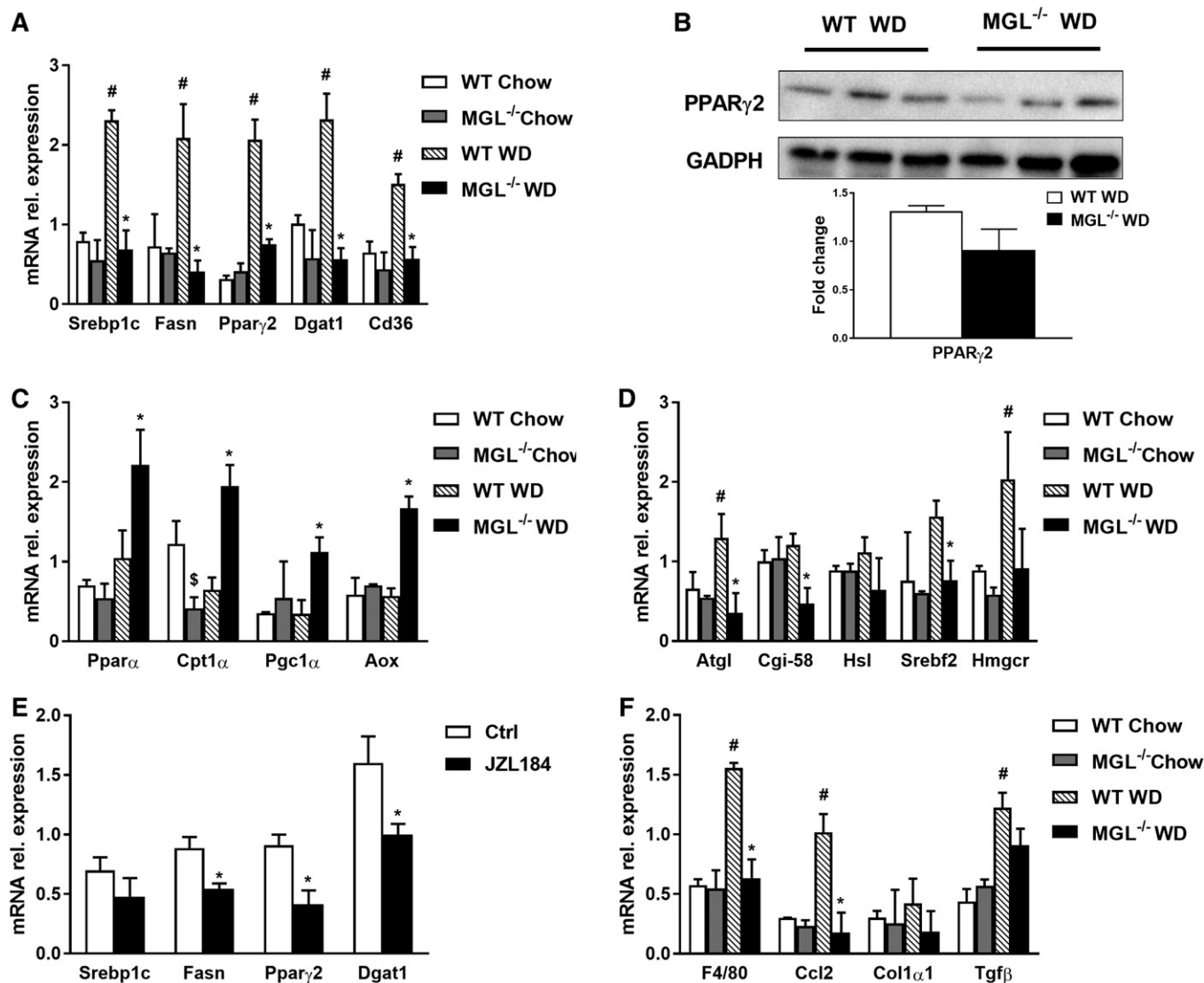


Fig. 2. MGL deficiency interferes with lipid metabolic pathways and reduces inflammation in liver. **A:** mRNA expression of genes controlling TG synthesis such as *Srebp1c*, *Fasn*, *Ppar γ 2*, *Dgat1*, and *Cd36* decreased. **B:** However, protein abundance of PPAR γ 2 showed no significant changes in MGL^{-/-} mice fed a WD. **C:** mRNA expression of FA oxidation markers *Ppara*, *Cpt1 α* , *Pgc1 α* , and *Aox* profoundly increased. **D:** Lipolytic pathway *Atgl*, *Cgi-58*, and *Hsl* were downregulated, whereas Chol synthesis *Srebf2* decreased, and *Hmgcr* remained unchanged. **E:** mRNA expression of genes controlling TG metabolism such as *Fasn*, *Ppar γ 2*, and *Dgat1* decreased, whereas *Srebp1c* remained unchanged in primary hepatocytes treated with MGL inhibitor JZL184. **F:** Gene expression of the proinflammatory markers *F4/80* and *Ccl2* decreased, whereas fibrosis remained unchanged as evidenced by *Col1 α 1* and *Tgfb*. rel., relative. * $P \leq 0.05$, WT WD versus MGL^{-/-} WD or Ctrl versus JZL184-treated hepatocytes; # $P \leq 0.05$ WT WD versus WT chow; \$ $P \leq 0.05$ WT chow versus MGL^{-/-} chow.

Lack of MGL drives PPAR γ -dependent adipogenesis

To further explore fat storage in adipose depots as a potential mechanism preventing ectopic fat accumulation, we measured gWAT weight, which was increased in MGL^{-/-} compared with WT animals, as already shown in Fig. 1B. Adipocyte expansion was further evident from increased *mGPES1a* mRNA levels (supplemental Fig. S2A). Gene expression involved in, respectively, FA storage, lipolysis, and synthesis was increased in MGL^{-/-} mice as demonstrated by *Ppar γ 2*, *Cd36*, *Atgl*, *Hsl*, *Fasn*, and *Dgat1* (Fig. 3A), together with *leptin* and *adiponectin* (Fig. 3B). Adiponectin serum levels were increased in MGL^{-/-} mice fed a WD (Fig. 3C), whereas genes involved in mitochondrial β -oxidation such as *Ppar α* remained unchanged, and *Cpt1 α* decreased in

gWAT (Fig. 3D). Importantly, inflammation was diminished in gWAT from MGL^{-/-} mice, as reflected by *Ccl2* and *Tnfa* gene expression (Fig. 3E) and diminished crown-like structures on Mac-2 staining (Fig. 3F). Notably, subcutaneous white AT (sWAT) weight increased in MGL^{-/-} mice (supplemental Fig. S2B), and FA synthesis pathways increased for *Dgat1* and remained unchanged for *Ppar γ 2* and *Cd36*, whereas inflammation strongly diminished in the MGL^{-/-} sWAT depot (supplemental Fig. S2C). Furthermore, PPAR α signature remained unremarkable in brown AT (BAT), whereas uncoupling protein 1 gene expression increased after WD feeding in MGL^{-/-} mice (supplemental Fig. S2D).

Because our data suggested that global MGL deficiency may promote adipogenesis and TG storage capacity in gWAT

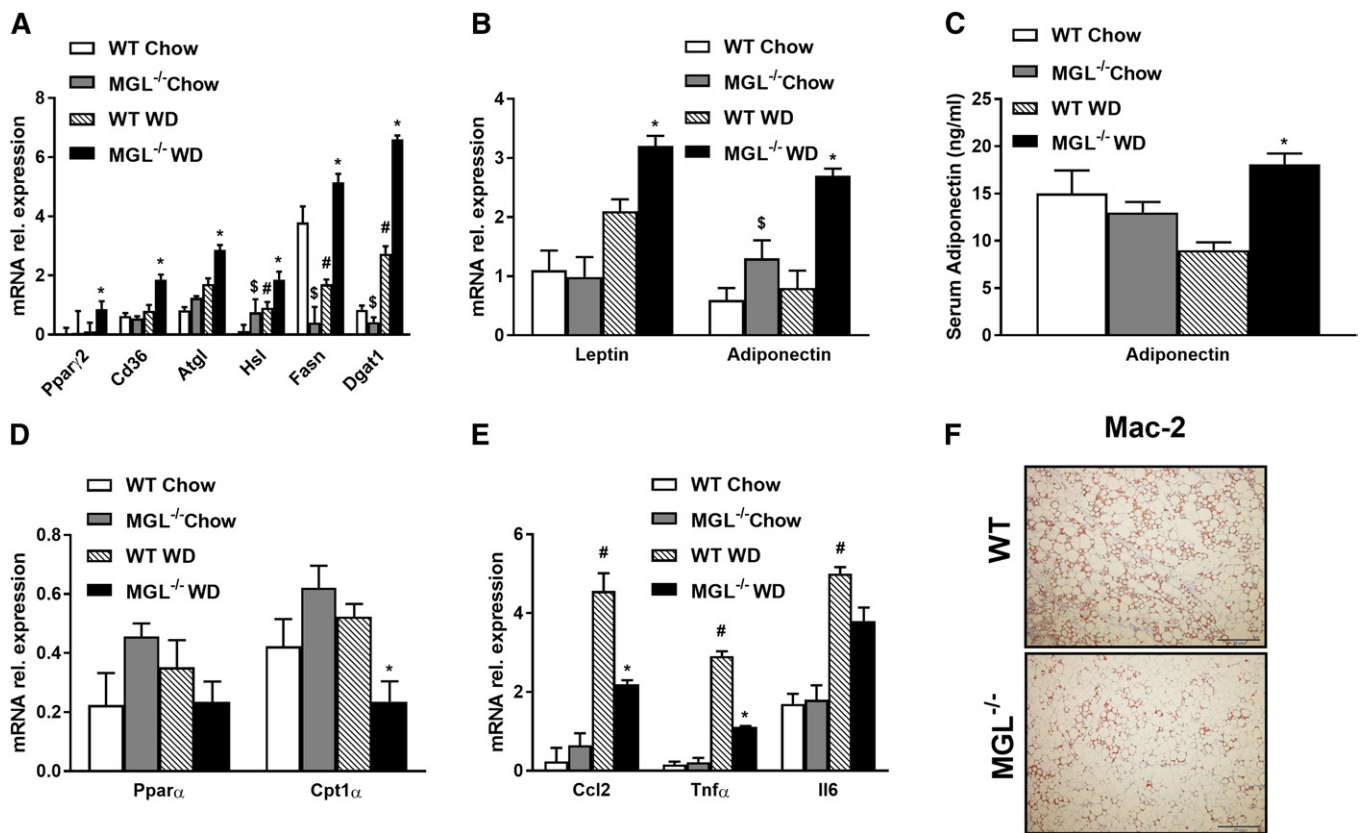


Fig. 3. Lack of MGL prevents ectopic lipid accumulation by gWAT storage, reducing AT inflammation. A: Adipose mRNA expression of genes controlling TG synthesis such as *Pparγ2*, *Cd36*, *Atgl*, *Hsl*, *Fasn*, and *Dgat1* were strongly increased. Gene expression profile of *leptin* and *adiponectin* increased together (B) with adiponectin quantification in plasma (C). *Ppara* and *Cpt1a* (D) and inflammatory markers *Ccl2*, *Tnfα*, and *Il6* (E) were diminished in *MGL^{-/-}* mice, in line with representative Mac-2 staining for gWAT sections (F). rel., relative. * $P \leq 0.05$, WT WD versus *MGL^{-/-}* WD; # $P \leq 0.05$ WT WD versus WT chow; § $P \leq 0.05$ WT chow versus *MGL^{-/-}* chow.

in vivo, we next used the 3T3-L1 cell line and differentiated them into full adipocytes during a time course of 13 days (16, 17). Interestingly, *Mgl* expression peaked at day 9 (Fig. 4A), whereas *Pparγ* peaked at day 13. We next used 3T3-L1 cells to perform MGL inhibition with JZL184, which strongly upregulated *Pparγ2*, *leptin*, and *adiponectin* (Fig. 4B) and therefore augmenting lipid storage and cell size as shown in the flow cytometry analysis (Fig. 4C). Furthermore, we verified this observation in APCs isolated from the stroma-vascular fraction of WT (Fig. 4D) and *MGL^{-/-}* mice (Fig. 4E). Interestingly, progenitor cells from *MGL^{-/-}* mice displayed higher potential to differentiate into mature adipocytes as evidenced by enhanced expression of adipogenic markers (in *MGL^{-/-}* preadipocytes such as *Dgat1*, *Pparγ2*, and *adiponectin*; Fig. 4E) together with increased lipid content and cell size in the BODIPY flow cytometric analysis (supplemental Fig. S2E). Characterization of APCs from WT and *MGL^{-/-}* mice further showed a non-significant reduction for PPAR γ (Fig. 4F). Because *Pparγ2* gene expression upregulated in 3T3-L1 cells upon JZL184 treatment and in APC differentiation, we aimed at investigating the ability of PPAR γ to regulate MGL expression. Fully differentiated 3T3-L1 adipocytes were treated with known PPAR γ agonists such as pio and rosi, both at a 10 μ M concentration for 48 h. Strikingly, *Mgl* mRNA expression was significantly increased by the PPAR γ agonist rosi,

together with *Pparγ2* and *Cd36* (Fig. 4G), whereas the less potent PPAR γ agonist pio induced *Cd36* but failed to increase *Pparγ2* and *Mgl* mRNA expression (Fig. 4G). To determine whether the induction of MGL expression was mediated by PPAR γ , 3T3-L1 cells were treated with the PPAR γ -specific antagonist GW-9662. Fully differentiated 3T3-L1 adipocytes were pretreated with GW-9662 (10 μ M) for 12 h, followed by treatment with 10 μ M GW-9662 alone or 100 nM rosi plus 10 μ M GW-9662 for an additional 24 h as previously performed by others (27). Treatment with GW-9662 inhibited rosi-mediated induction of *Mgl* mRNA expression (Fig. 4H). Together, these data show that MGL deficiency promotes adipogenic differentiation in 3T3-L1 cells, primary APCs in vitro, and gWAT in vivo, being regulated by PPAR γ in the feedback loop. Therefore, MGL deletion could possibly create a futile cycle whereby part of the products of TG hydrolysis can be recycled within the cell, while FAs activate PPAR γ , which promotes adiponectin secretion to the liver and releases FAs, activating hepatic PPAR α via ATGL (Fig. 5).

DISCUSSION

Hepatic lipid accumulation results from an imbalance between lipid uptake/lipogenesis and lipid oxidation or

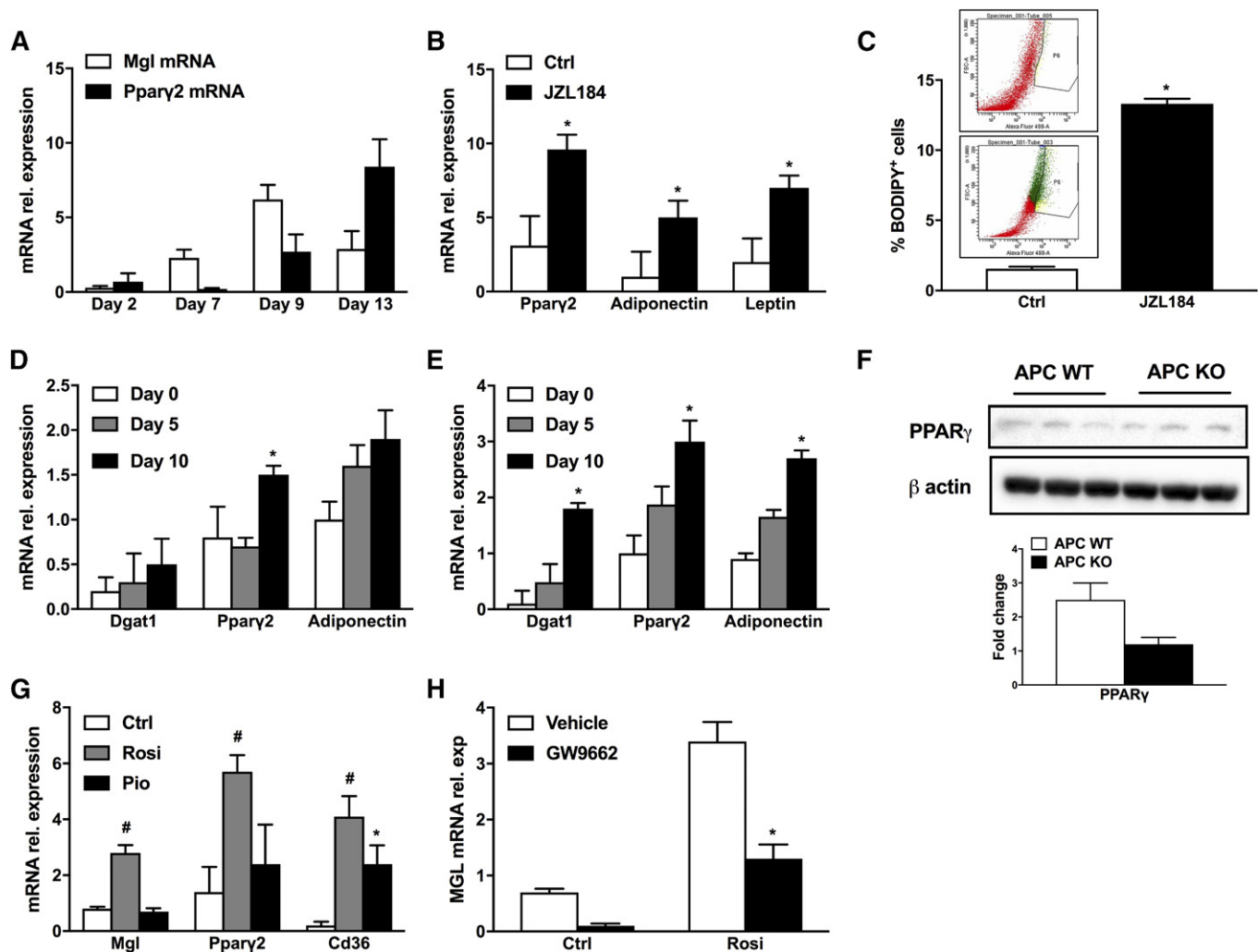


Fig. 4. MGL inhibition promotes lipid storage in 3T3-L1 cells and APCs via PPAR γ regulation. **A:** *Mgl* and *Ppary2* gene expression during 3T3-L1 differentiation time course (13 days). **B:** mRNA gene expression of *Ppary2*, *adiponectin*, and *leptin* after JZL184 treatment resulted in augmented expression of lipogenic genes. **C:** BODIPY flow cytometry staining of nontreated (Ctrl) and JZL184-treated 3T3-L1 cells with representative dot plots demonstrates increased lipid content. mRNA gene expression analysis of adipogenic genes *Dgat1*, *Ppary2*, and *adiponectin* in APCs isolated from WT animals (**D**) and APCs from MGL $^{-/-}$ mice upregulated (**E**). **F:** Protein expression of PPAR γ and β -actin with densitometric analysis. **G:** mRNA gene expression of *Mgl*, *Ppary2*, and *Cd36* of 3T3-L1 cells treated with rosi or pio for 48 h significantly increased. **H:** MGL mRNA relative (rel.) expression of fully differentiated 3T3L1 treated with GW9662 alone (a potent antagonist of PPAR γ) or in combination with rosi. Mean of three independent experiments \pm SD value. * $P \leq 0.05$, treatment versus control; # rosiglitazone versus control.

lipoprotein secretion, which eventually triggers lipotoxicity and hepatic injury (28). Indeed, NAFLD is considered as the hepatic manifestation of metabolic syndrome and is typically associated with insulin resistance (29), promoting FA flux to the liver. MGL genetic and pharmacological inhibition was shown to protect against inflammation and liver lesions induced by ischemia/reperfusion injury (30). In addition, we recently showed that MGL invalidation strongly decreases fibrogenesis due to autophagy-mediated antiinflammatory properties in macrophages (31). Moreover, MGL expression is increased in intestine and liver by HFD treatment, indicating a potential role of MGs in intestinal degradation and absorption (8, 25, 32). Taschler et al. (8) found accumulation of several MG species after HFD challenge; interestingly, 18:2 and 20:4 MG accumulated in the liver as well as in the gWAT but not in the small intestine of MGL $^{-/-}$ mice. Notably, transgenic overexpression

of MGL in the intestine resulted in weight gain, hyperphagia, and augmented FA oxidation in comparison to WT (33). However, a functional role of MGL in obesity-associated hepatic steatosis still remains controversial. Although some studies showed that MGL-deficient mice were leaner at baseline (34) or gained more weight when fed a HFD despite better insulin resistance (8), others reported diminished weight gain on a HFD compared with their WT controls (7). Therefore, we hypothesized that targeting MGL may reprogram lipid metabolism, thus counteracting NAFLD progression.

Our data highlight novel functions of MGL in the pathogenesis of NAFLD. MGL deficiency in mice protected from hepatic steatosis and weight gain after 12 weeks of feeding with an obesogenic WD (Fig. 1). Expression of marker genes indicated decreased hepatic production of *Ppary2* in MGL $^{-/-}$ mice, perhaps because of decreased de novo

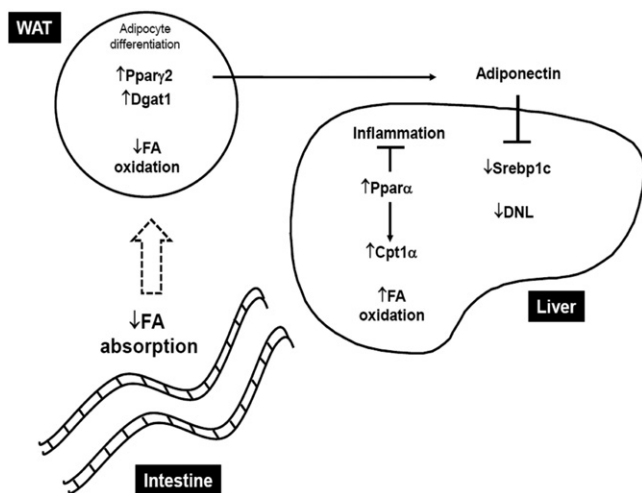


Fig. 5. Lack of MGL prevents hepatic steatosis by favoring lipid storage in AT and intestinal malabsorption. MGL deficiency determines intestinal malabsorption, which delivers less FAs to the peripheral tissues. In adipocytes, a large portion of FA is hydrolyzed and reesterified to TGs in a futile cycle with upregulation of lipogenic genes such as *Pparγ2* and *Dgat1*. This translates into increased adiponectin production, resulting in diminished de novo lipogenesis (DNL) in the liver as indicated by downregulation of *Srebp1c* and increased hepatic FA oxidation (*Pparα* and its target *Cpt1α*) and less hepatic inflammation. WAT, white AT.

lipogenesis and *Srebp1c/Fasn* expression, coupled with increased FA oxidation mediated by *PPARα* (Fig. 2). Consequently, the expression of *Dgat1*, which is regulated by *PPARγ* and catalyzes TG formation (26), was significantly decreased in the liver (Fig. 2A). Thus, reduced hepatic TG synthesis was also accompanied by relatively increased β oxidation, therefore contributing to diminished steatosis in *MGL^{-/-}* mice.

Notably, plasma NEFAs were preferentially distributed toward nonhepatic tissue in *MGL^{-/-}* animals, suggesting changes in lipid partition/fluxes. Indeed, gWAT as well as sWAT weight was strikingly increased in WD-fed *MGL^{-/-}* mice (Fig. 1B, supplemental Fig. S2B), indicating that MGL deficiency facilitates fat storage in AT, thereby preventing its ectopic accumulation in the liver. Interestingly, the increased gWAT weight in *MGL^{-/-}* mice was also demonstrated by Douglass et al. (7), but not by Taschler et al (8). In our hands, MGL deficiency resulted in white AT expansion in both gonadal and subcutaneous depot (Fig. 1B, supplemental Fig. S2B), whereas *PPARγ2* signaling was increased only in gWAT (Fig. 3A) but not in sWAT (supplemental Fig. S2C). These findings highlight the physiological differences between MGL inhibition and *PPARγ* agonists, because glitazones are known to increase body weight exclusively via sWAT expansion (35). In addition, decreased inflammatory alterations in gWAT (Fig. 3E, F) and sWAT of obese *MGL^{-/-}* mice (supplemental Fig. S2C) could contribute to fewer metabolic perturbations following AT enlargement. Obesity-mediated hepatic inflammation and macrophage accumulation were diminished in liver from *MGL^{-/-}* animals, together with increased lipid accumulation in gWAT instead of liver and diminished AT inflammation.

The antiinflammatory effects of MGL deficiency may prime adipogenesis, leading to the observed healthier

expansion of AT in *MGL^{-/-}* animals. These proadipogenic alterations are demonstrated in vitro in 3T3-L1 cells and gWAT-derived APCs. Strikingly, the involvement of *PPARγ* is supported by increased MGL expression after agonism with rosi. *PPARγ* was shown to regulate many adipocyte genes involved in lipid metabolism and energy balance (36, 37), generally promoting FA storage. Furthermore, previous studies have demonstrated that ATGL was controlled by the *PPARγ* feedback loop in 3T3-L1 cells (27). Therefore, to demonstrate that *PPARγ* was mediating the positive response of rosi on *Mgl* mRNA expression, we combined rosi with GW-9662. GW-9662 is a potent antagonist of *PPARγ* via irreversible covalent modification of a cysteine residue in the *PPARγ* ligand-binding domain (38). Importantly, GW-9662 antagonism inhibited rosi-mediated induction of *Mgl* mRNA expression in 3T3L1 cells, proving *PPARγ* regulation of MGL expression at the gene level (Fig. 4G, H).

The discrepancy between diminished body and augmented adipose fat weight turned our attention to investigate intestinal malabsorption as a possible mechanistic explanation for our findings. Intestinal malabsorption was already described in a recent study, in which Vujic et al. (25) crossed *ApoE^{-/-}* with *MGL^{-/-}* mice to potentiate the effects of disrupted lipid signaling and exacerbate hyperlipidemia. In addition, it was shown that delayed gastric emptying and reduced gut motility may contribute to reduced FA uptake and Chol absorption in double-KO animals (25). In line with this report, we also investigated intestinal fat absorption in our model and observed elevated FA content in the feces, which we confirmed with gas-chromatography analysis after sucrose polybehenate feeding, evidencing reduced lipid absorption in *MGL^{-/-}* mice fed a WD.

Altogether, at least two mechanisms are likely to contribute to the improvement of obesity-related hepatic steatosis and metabolic perturbation upon MGL deficiency. On one hand, lack of MGL may facilitate lipid storage in AT via *PPARγ* feedback regulation, thereby reducing hepatic TG accumulation/inflammation. On the other hand, intestinal FA malabsorption favored by MGL deletion explains body weight differences between WD-fed mice. Thus, MGL deletion creates a futile cycle of lipolysis in AT, resulting in a marked diminution of FA release from adipocytes as well as generation of FAs able to activate *PPARγ*. Blocking MGL effects in vivo could normalize altered hepatic lipid homeostasis in obesity and therefore prevent progression of NAFLD. However, characterization of the function and regulation of MGL and/or other lipases such as adiponutrin remains to be determined. Moreover, the precise role of MGL and its regulation by *PPARγ* in adipocyte lipid homeostasis requires further evaluation.

In conclusion, our data uncover that MGL deletion prevents steatosis by promoting lipid storage in gWAT and FA malabsorption, resulting in a leaner phenotype. **FIG**

The authors thank Dr. Veronica Moreno-Viedma (Institute of Cancer Research, Medical University of Vienna) for excellent technical support and Dr. Patrick Starlinger (Department of Surgery, Medical University of Vienna) for support with primary hepatocyte isolation from human livers.

REFERENCES

1. Younossi, Z., Q. M. Anstee, M. Marietti, T. Hardy, L. Henry, M. Eslam, J. George, and E. Bugianesi. 2018. Global burden of NAFLD and NASH: trends, predictions, risk factors and prevention. *Nat. Rev. Gastroenterol. Hepatol.* **15**: 11–20.
2. Benedict, M., and X. Zhang. 2017. Non-alcoholic fatty liver disease: an expanded review. *World J. Hepatol.* **9**: 715–732.
3. Estes, C., H. Razavi, R. Loomba, Z. Younossi, and A. J. Sanyal. 2018. Modeling the epidemic of nonalcoholic fatty liver disease demonstrates an exponential increase in burden of disease. *Hepatology.* **67**: 123–133.
4. Musso, G., R. Gambino, and M. Cassader. 2009. Recent insights into hepatic lipid metabolism in non-alcoholic fatty liver disease (NAFLD). *Prog. Lipid Res.* **48**: 1–26.
5. Poursharifi, P., S. R. M. Madiraju, and M. Prentki. 2017. Monoacylglycerol signalling and ABHD6 in health and disease. *Diabetes Obes. Metab.* **19**: 76–89.
6. Long, J. Z., W. Li, L. Booker, J. J. Burston, S. G. Kinsey, J. E. Schlosburg, F. J. Pavón, A. M. Serrano, D. E. Selley, L. H. Parsons, et al. 2009. Selective blockade of 2-arachidonoylglycerol hydrolysis produces cannabinoid behavioral effects. *Nat. Chem. Biol.* **5**: 37–44.
7. Douglass, J. D., Y. X. Zhou, A. Wu, J. A. Zadrogra, A. M. Gajda, A. I. Lackey, W. Lang, K. M. Chevalier, S. W. Sutton, S-P. Zhang, et al. 2015. Global deletion of MGL in mice delays lipid absorption and alters energy homeostasis and diet-induced obesity. *J. Lipid Res.* **56**: 1153–1171.
8. Taschler, U., F. P. W. Radner, C. Heier, R. Schreiber, M. Schweiger, G. Schoiswohl, K. Preiss-Landl, D. Jaeger, B. Reiter, H. C. Koefeler, et al. 2011. Monoglyceride lipase deficiency in mice impairs lipolysis and attenuates diet-induced insulin resistance. *J. Biol. Chem.* **286**: 17467–17477.
9. Fickert, P., G. Zollner, A. Fuchsichler, C. Stumptner, A. H. Weiglein, F. Lammert, H. U. Marschall, O. Tsybrovskyy, K. Zatloukal, H. Denk, et al. 2002. Ursodeoxycholic acid aggravates bile infarcts in bile duct-ligated and Mdr2 knockout mice via disruption of cholangioles. *Gastroenterology.* **123**: 1238–1251.
10. Fickert, P., A. Fuchsichler, M. Wagner, G. Zollner, A. Kaser, H. Tilg, R. Krause, F. Lammert, C. Langner, K. Zatloukal, et al. 2004. Regurgitation of bile acids from leaky bile ducts causes sclerosing cholangitis in Mdr2 (Abcb4) knockout mice. *Gastroenterology.* **127**: 261–274.
11. Fuchs, C. D., G. Paumgartner, V. Mlitz, V. Kunczer, E. Halilbasic, N. Leditznig, A. Wahlström, M. Ståhlman, A. Thüringer, K. Kashofer, et al. 2018. Colesevelam attenuates cholestatic liver and bile duct injury in *Mdr2*^{-/-} mice by modulating composition, signalling and excretion of faecal bile acids. *Gut.* **67**: 1683–1691.
12. Bruschi, F. V., T. Claudel, M. Tardelli, A. Caligiuri, T. M. Stulnig, F. Marra, and M. Trauner. 2017. The PNPLA3 I148M variant modulates the fibrogenic phenotype of human hepatic stellate cells. *Hepatology.* **65**: 1875–1890.
13. Bhogal, R. H., J. Hodson, D. C. Bartlett, C. J. Weston, S. M. Curbishley, E. Haughton, K. T. Williams, G. M. Reynolds, P. N. Newsome, D. H. Adams, et al. 2011. Isolation of primary human hepatocytes from normal and diseased liver tissue: a one hundred liver experience. *PLoS One.* **6**: e18222.
14. Moreno-Viedma, V., M. Tardelli, M. Zeyda, M. Sibilia, J. D. Burks, and M. T. Stulnig. 2018. Osteopontin-deficient progenitor cells display enhanced differentiation to adipocytes. *Obes. Res. Clin. Pract.* **12**: 277–285.
15. Rodeheffer, M. S., K. Birsoy, and J. M. Friedman. 2008. Identification of white adipocyte progenitor cells in vivo. *Cell.* **135**: 240–249.
16. Madsen, L., R. K. Petersen, M. B. Sørensen, C. Jørgensen, P. Hallenborg, L. Pridal, J. Fleckner, E. Z. Amri, P. Krieg, G. Furstemberger, et al. 2003. Adipocyte differentiation of 3T3-L1 pre-adipocytes is dependent on lipoxigenase activity during the initial stages of the differentiation process. *Biochem. J.* **375**: 539–549.
17. Neal, J. W., and N. A. Clipstone. 2002. Calcineurin mediates the calcium-dependent inhibition of adipocyte differentiation in 3T3-L1 cells. *J. Biol. Chem.* **277**: 49776–49781.
18. Tardelli, M., T. Claudel, F. V. Bruschi, V. Moreno-Viedma, and M. Trauner. 2017. Adiponectin regulates AQP3 via PPAR α in human hepatic stellate cells. *Biochem. Biophys. Res. Commun.* **490**: 51–54.
19. Spangenburg, E. E., S. J. P. Pratt, L. M. Wohlers, and R. M. Lovering. 2011. Use of BODIPY (493/503) to visualize intramuscular lipid droplets in skeletal muscle. *J. Biomed. Biotechnol.* **2011**: 598358.
20. Tardelli, M., V. Moreno-Viedma, M. Zeyda, B. K. Itariu, F. B. Langer, G. Prager, and T. M. Stulnig. 2017. Adiponectin regulates aquaglyceroporin expression in hepatic stellate cells altering their functional state. *J. Gastroenterol. Hepatol.* **32**: 253–260.
21. Jandacek, R. J., J. E. Heubi, and P. Tso. 2004. A novel, noninvasive method for the measurement of intestinal fat absorption. *Gastroenterology.* **127**: 139–144.
22. Adlof, R. O. 2003. Advances in Lipid Methodology, Oily Press Lipid Library Series. R. O. Adlof, editor. Vol. 5, Chapter 2. Elsevier. 69–111.
23. Schweiger, M., M. Romauch, R. Schreiber, G. F. Grabner, S. Hütter, P. Kotzbeck, P. Benedikt, T. O. Eichmann, S. Yamada, O. Knittelfelder, et al. 2017. Pharmacological inhibition of adipose triglyceride lipase corrects high-fat diet-induced insulin resistance and hepatosteatosis in mice. *Nat. Commun.* **8**: 14859.
24. Scherer, P. E. 2006. Adipose tissue: from lipid storage compartment to endocrine organ. *Diabetes.* **55**: 1537–1545.
25. Vujic, N., M. Korbelius, C. Leopold, M. Duta-Mare, S. Rainer, S. Schlager, M. Goeritzer, D. Kolb, T. O. Eichmann, C. Diwoy, et al. 2017. Monoglyceride lipase deficiency affects hepatic cholesterol metabolism and lipid-dependent gut transit in ApoE^{-/-} mice. *Oncotarget.* **8**: 33122–33136.
26. Harris, C. A., J. T. Haas, R. S. Streeper, S. J. Stone, M. Kumari, K. Yang, X. Han, N. Brownell, R. W. Gross, R. Zechner, et al. 2011. DGAT enzymes are required for triacylglycerol synthesis and lipid droplets in adipocytes. *J. Lipid Res.* **52**: 657–667.
27. Kershaw, E. E., M. Schupp, H-P. Guan, N. P. Gardner, M. A. Lazar, and J. S. Flier. 2007. PPAR regulates adipose triglyceride lipase in adipocytes in vitro and in vivo. *Am. J. Physiol. Endocrinol. Metab.* **293**: E1736–E1745.
28. Trauner, M., M. Arrese, and M. Wagner. 2010. Fatty liver and lipotoxicity. *Biochim. Biophys. Acta.* **1801**: 299–310.
29. Angulo, P. 2002. Nonalcoholic fatty liver disease. *N. Engl. J. Med.* **346**: 1221–1231.
30. Cao, Z., M. M. Mulvihill, P. Mukhopadhyay, H. Xu, K. Erdélyi, E. Hao, E. Holovac, G. Haskó, B. F. Cravatt, D. K. Nomura, et al. 2013. Monoacylglycerol lipase controls endocannabinoid and eicosanoid signaling and hepatic injury in mice. *Gastroenterology.* **144**: 808–817. e15.
31. Habib, A., D. Chokr, J. Wan, P. Hegde, M. Mabire, M. Siebert, L. Ribeiro-Parenti, M. Le Gall, P. Lettéron, N. Pilard, et al. Inhibition of monoacylglycerol lipase, an anti-inflammatory and antifibrogenic strategy in the liver. *Gut.* Epub ahead of print. October 9, 2018; doi:10.1136/gutjnl-2018-316137.
32. Duncan, M., A. D. Thomas, N. L. Cluny, A. Patel, K. D. Patel, B. Lutz, D. Piomelli, S. P. H. Alexander, K. A. Sharkey, B. Lutz, et al. 2008. Distribution and function of monoacylglycerol lipase in the gastrointestinal tract. *Am. J. Physiol. Gastrointest. Liver Physiol.* **295**: G1255–G1265.
33. Chon, S. H., J. D. Douglass, Y. X. Zhou, N. Malik, J. L. Dixon, A. Brinker, L. Quadro, and J. Storch. 2012. Over-expression of monoacylglycerol lipase (MGL) in small intestine alters endocannabinoid levels and whole body energy balance, resulting in obesity. *PLoS One.* **7**: e43962.
34. Chanda, P. K., Y. Gao, L. Mark, J. Btsh, B. W. Strassle, P. Lu, M. J. Piesla, M-Y. Zhang, B. Bingham, A. Uveges, et al. 2010. Monoacylglycerol lipase activity is a critical modulator of the tone and integrity of the endocannabinoid system. *Mol. Pharmacol.* **78**: 996–1003.
35. Bays, H., L. Mandarino, and R. A. DeFronzo. 2004. Role of the adipocyte, free fatty acids, and ectopic fat in pathogenesis of type 2 diabetes mellitus: peroxisomal proliferator-activated receptor agonists provide a rational therapeutic approach. *J. Clin. Endocrinol. Metab.* **89**: 463–478.
36. Delerive, P., J. C. Fruchart, and B. Staels. 2001. Peroxisome proliferator-activated receptors in inflammation control. *J. Endocrinol.* **169**: 453–459.
37. Desvergne, B., and W. Wahli. 1999. Peroxisome proliferator-activated receptors: nuclear control of metabolism. *Endocr. Rev.* **20**: 649–688.
38. Leesnitzer, L. M., D. J. Parks, R. K. Bledsoe, J. E. Cobb, J. L. Collins, T. G. Consler, R. G. Davis, E. A. Hull-Ryde, J. M. Lenhard, L. Patel, et al. 2002. Functional consequences of cysteine modification in the ligand binding sites of peroxisome proliferator activated receptors by GW9662. *Biochemistry.* **41**: 6640–6650.